

**New anthrahydrazone derivatives and their cisplatin-like complexes:
Synthesis, antitumor activity and structure-activity relationship**

Rui-Xue Liu[†], Ying-Shu Wu[†], Yan-Cheng Liu^{}, Ru-Yi Luo, Li-Dong Yang, Meng-Ting Tang, Zhen-Feng Chen, Hong Liang^{*}*

State Key Laboratory for the Chemistry and Molecular Engineering of Medicinal Resources,
School of Chemistry & Pharmaceutical Sciences, Guangxi Normal University, Guilin, 541004, P.
R. China

[†] The authors contribute equally to this work.

*Corresponding authors' E-mail addresses: ycliu@gxnu.edu.cn (Y.-C. Liu);
hliang@gxnu.edu.cn (H. Liang); Tel./Fax: +86-773-2120958

Table S1. Selected bonds lengths and angles for the platinum(II) complexes **1** and **2**

Selected bond (Å)	
Pt complex 1	Pt complex 2
Pt1–Cl1	2.279(2)
Pt1–Cl2	2.289(2)
Pt1–N1	1.975(7)
Pt1–N4	2.001(6)
Selected angles (°)	
Pt complex 1	Pt complex 2
Cl1–Pt1–Cl2	88.80(9)
N1–Pt1–Cl1	95.9(2)
N1–Pt1–Cl2	175.26(19)
N1–Pt1–N4	80.2(3)
N3–N4–Pt1	112.4(4)
C3–N1–Pt1	129.6(7)
C12–C13–C14	122.4(8)
Cl1–Pt1–Cl2	89.06(5)
N1–Pt1–Cl1	95.78(11)
N1–Pt1–Cl2	175.14(11)
N1–Pt1–N4	80.61(14)
N3–N4–Pt1	112.4(2)
C3–N1–Pt1	129.4(3)
O1–C14–C13	123.1(5)

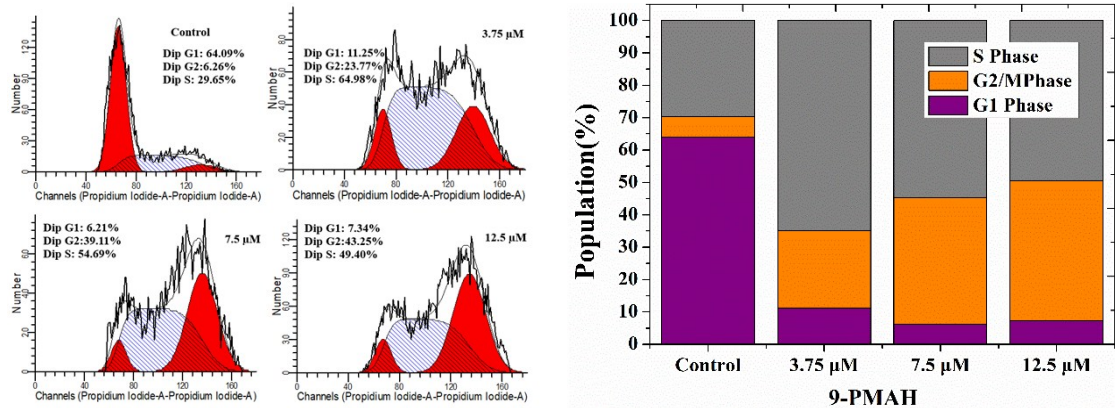


Figure S1. The percentages for the different phases of the cell cycle in T-24 cells arrested by **9-PMAH**.

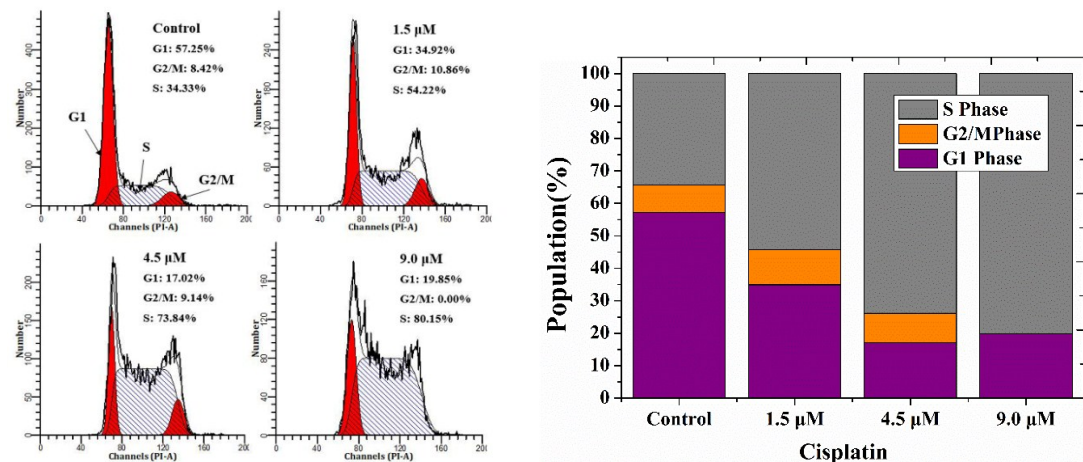


Figure S2. The percentages for the different phases of the cell cycle in T-24 cells arrested by **cisplatin**, with the same concentrations as 9-PMAH-Pt.

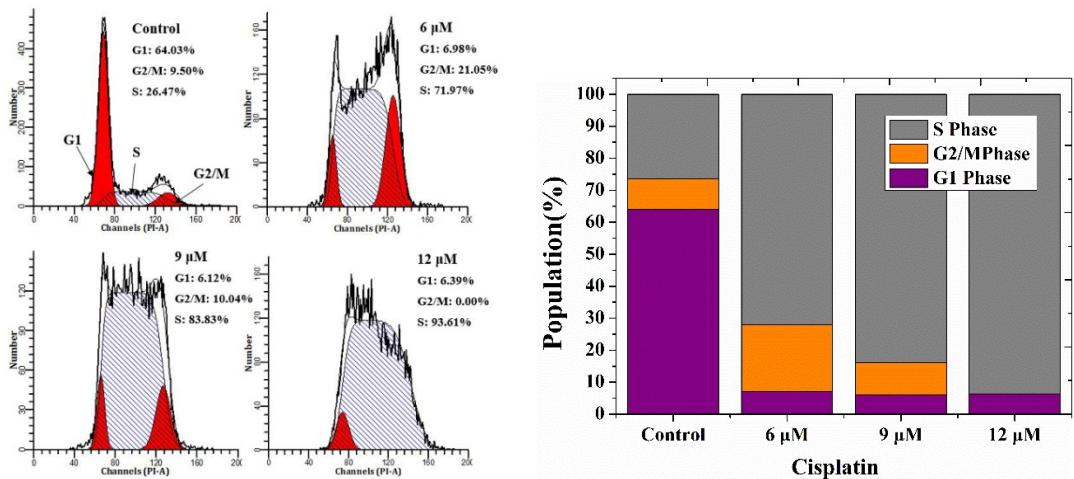


Figure S3. The percentages for the different phases of the cell cycle in MGC-803 cells arrested by **cisplatin**, with the same concentrations as 9-PMAH-Pt.

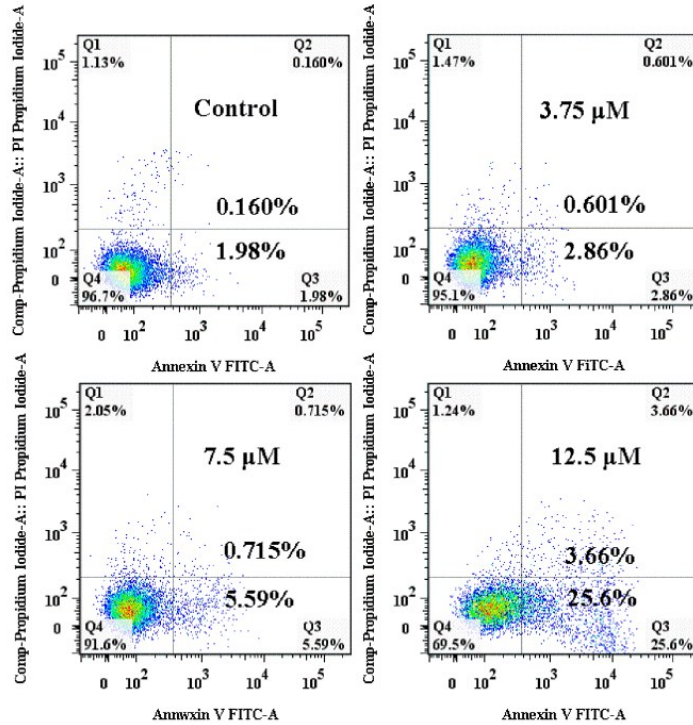


Figure S4. The cell apoptosis in T-24 cells induced by 9-PMAH in different concentrations related with IC₅₀ value.

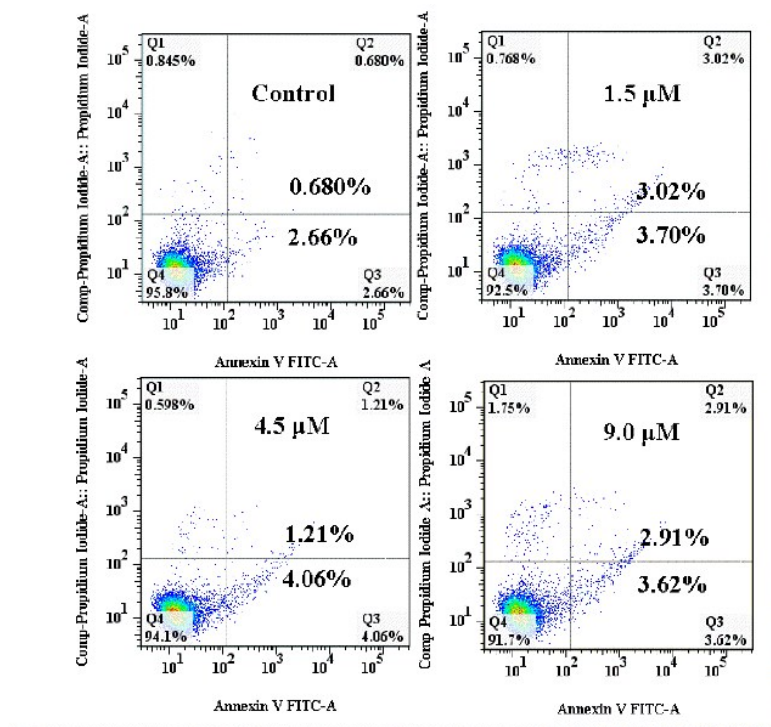


Figure S5. The cell apoptosis in T-24 cells induced by cisplatin, with the same concentrations as 9-PMAH-Pt

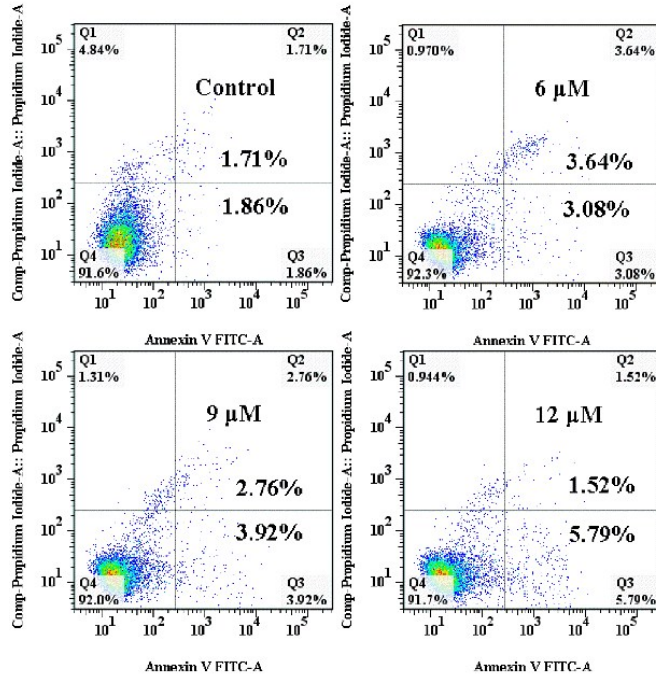


Figure S6. The cell apoptosis in MGC-803 cells induced by **cisplatin**, with the same concentrations as 9-PMAH-Pt

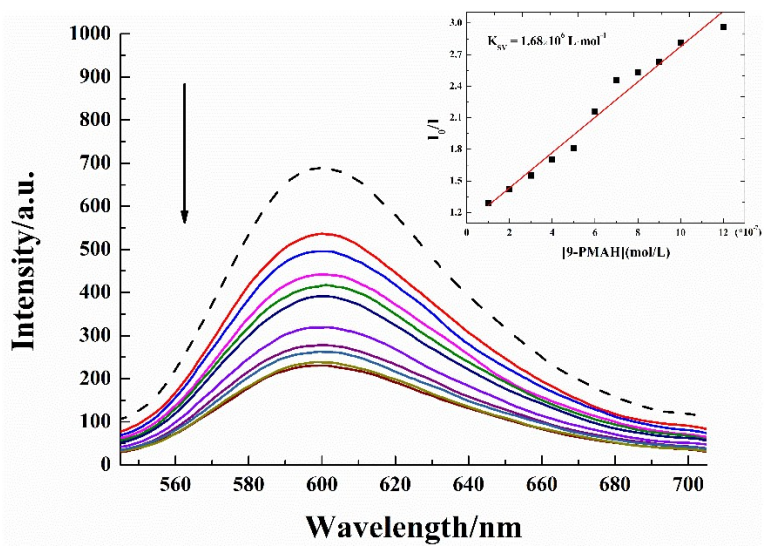


Figure S7. The fluorescence emission spectra of GR-DNA in the absence (dashed line) and the presence (solid lines) of 9-PMAH with increasing concentrations ([GR]/[DNA]/[9-PMAH] range from 1:10:0.01 to 1:10:0.09).

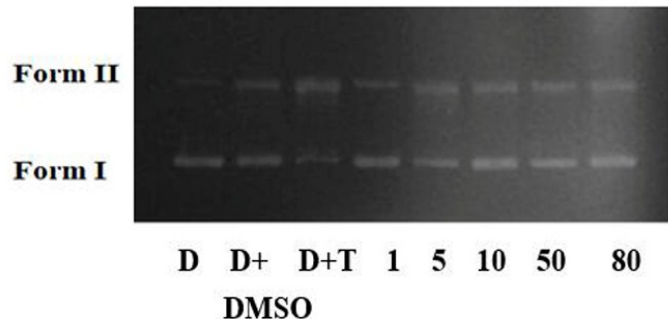
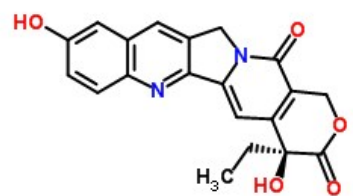
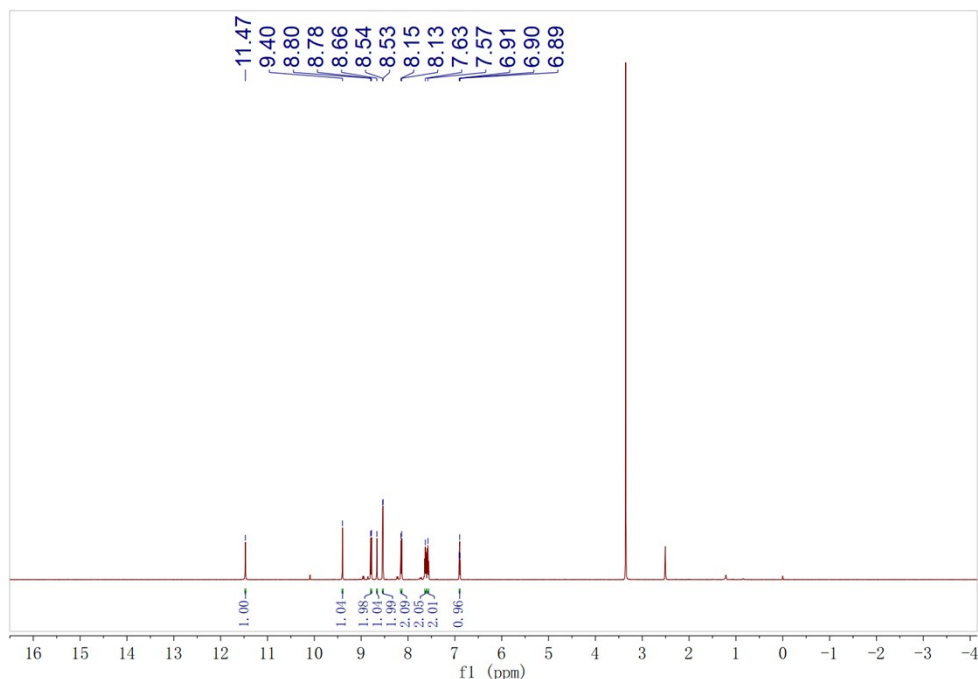


Figure S8. Inhibitory abilities of (S)-10-Hydroxycamptothecin on topoisomerase type I (Topo I)

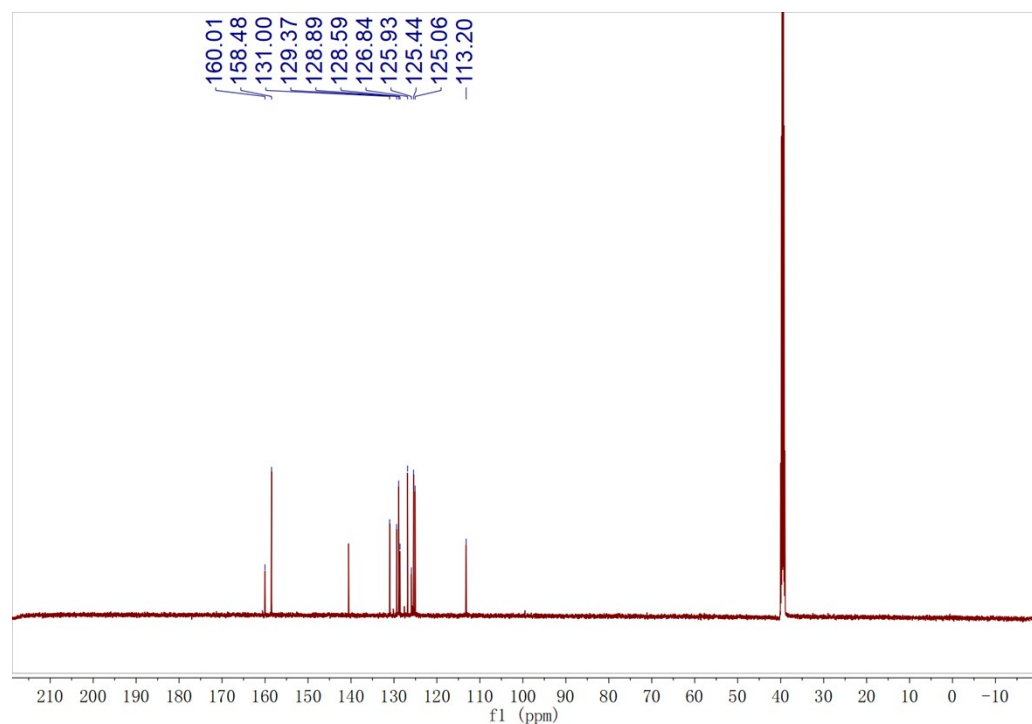


(S)-10-Hydroxycamptothecin

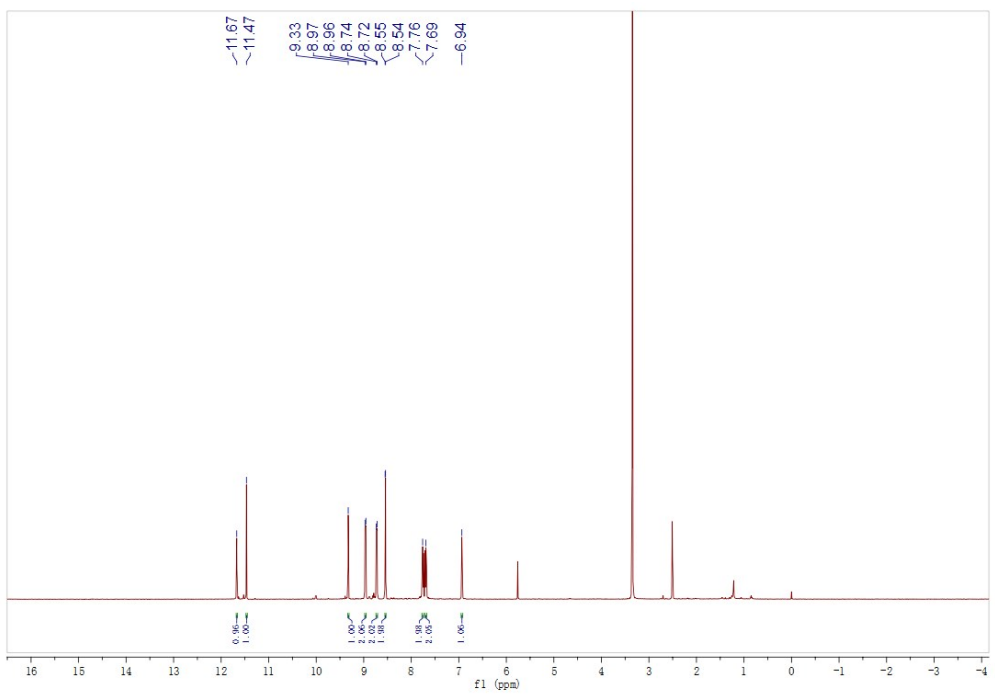
The spectral characterizations for both the ligands and both the Pt(II) complexes:



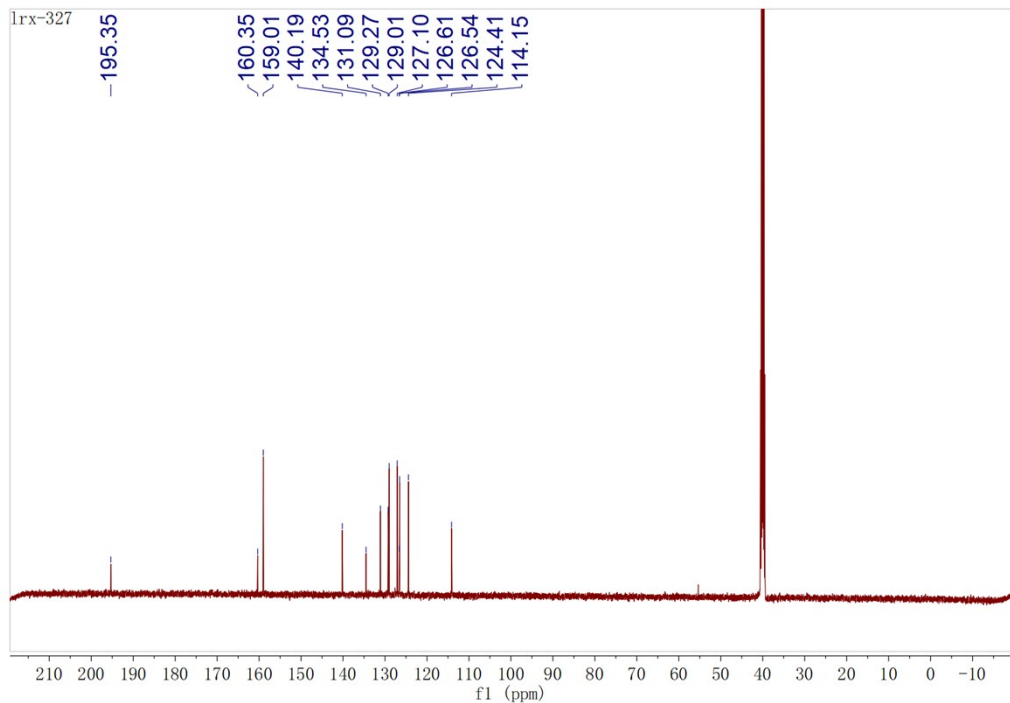
9-PMAH: ¹H-NMR (500 MHz, d_6 -DMSO) δ 11.47 (s, 1H), 9.40 (s, 1H), 8.79 (d, J =8.9 Hz, 2H), 8.66 (s, 1H), 8.54 (d, J =4.7 Hz, 2H), 8.14 (d, J =8.3 Hz, 2H), 7.63 (s, 2H), 7.57 (s, 2H), 6.90 (t, J =4.7 Hz, 1H).



9-PMAH: ¹³C-NMR (126 MHz, d_6 -DMSO) δ 160.01, 158.48, 140.55, 131.00, 129.37, 128.89, 128.59, 126.84, 125.93, 125.44, 125.06, 113.20.

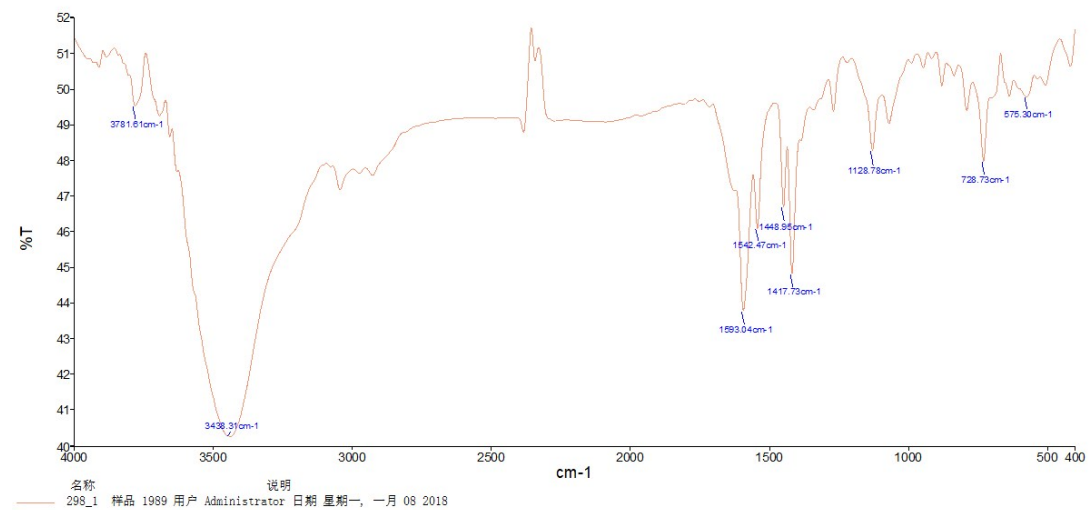


APMAH: ^1H NMR(500 MHz, d_6 -DMSO): δ 11.67 (s, 1H), 11.47 (s, 1H), 9.33 (s, 1H), 8.96 (d, J =8.8 Hz, 2H), 8.73 (d, J =8.8 Hz, 2H), 8.55 (d, J =4.8 Hz, 2H), 7.76 (s, 2H), 7.69 (s, 2H), 6.94 (t, J =4.5 Hz, 1H).

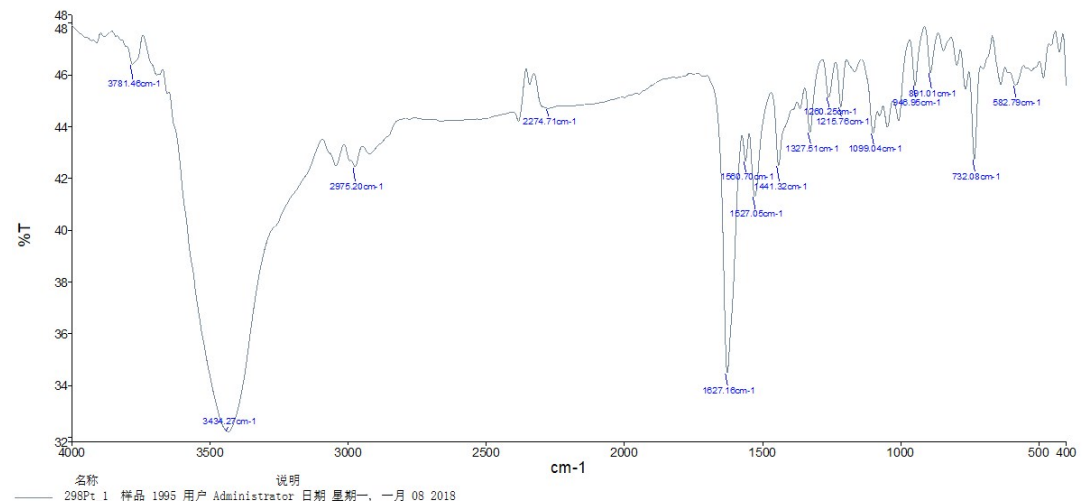


APMAH: ^{13}C NMR(126MHz, d_6 -DMSO): δ 195.35, 160.35, 159.01, 140.19, 134.53,

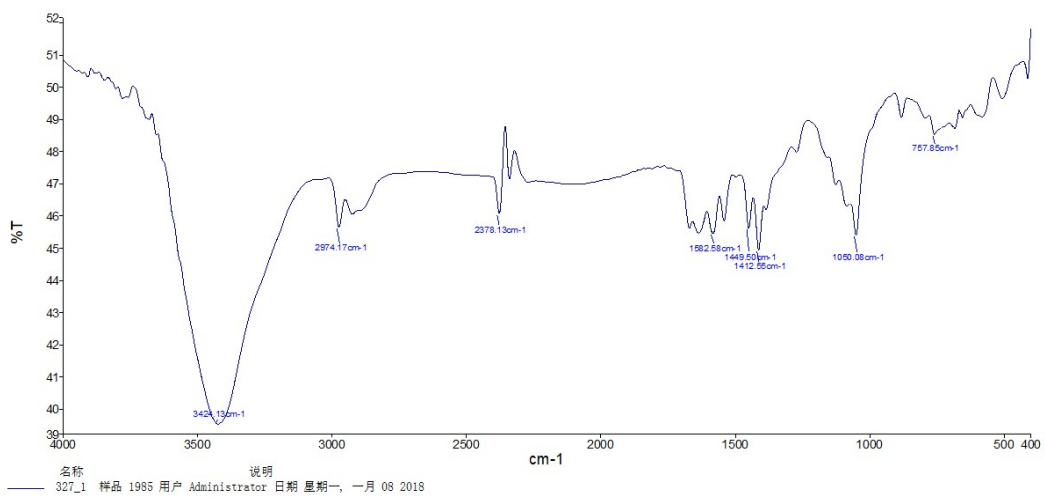
131.09, 129.27, 129.01, 127.10, 126.61, 126.54, 124.41, 114.15.



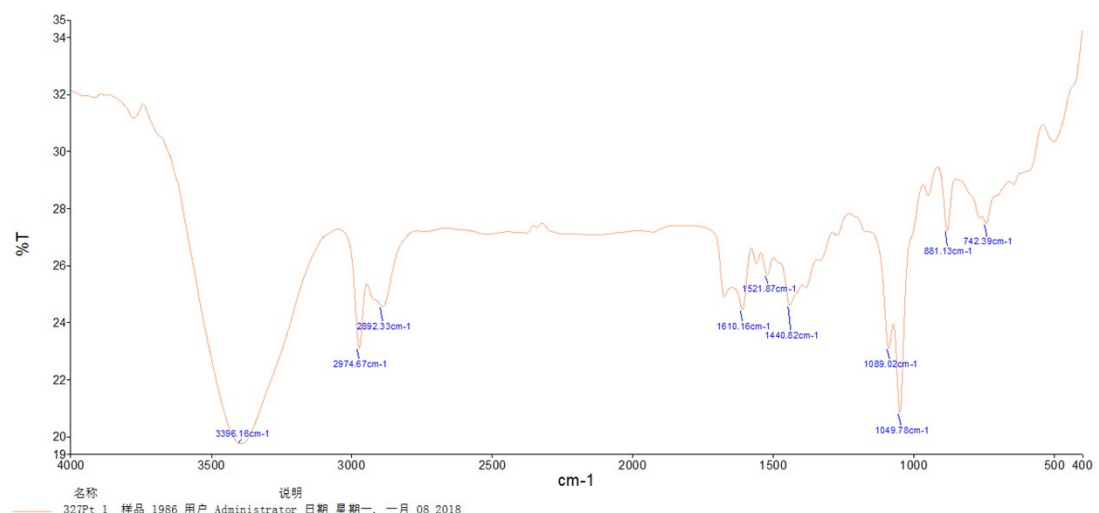
9-PMAH: IR (KBr): 3781, 3438, 1593, 1542, 1448, 1417, 1128, 728, 575 cm⁻¹



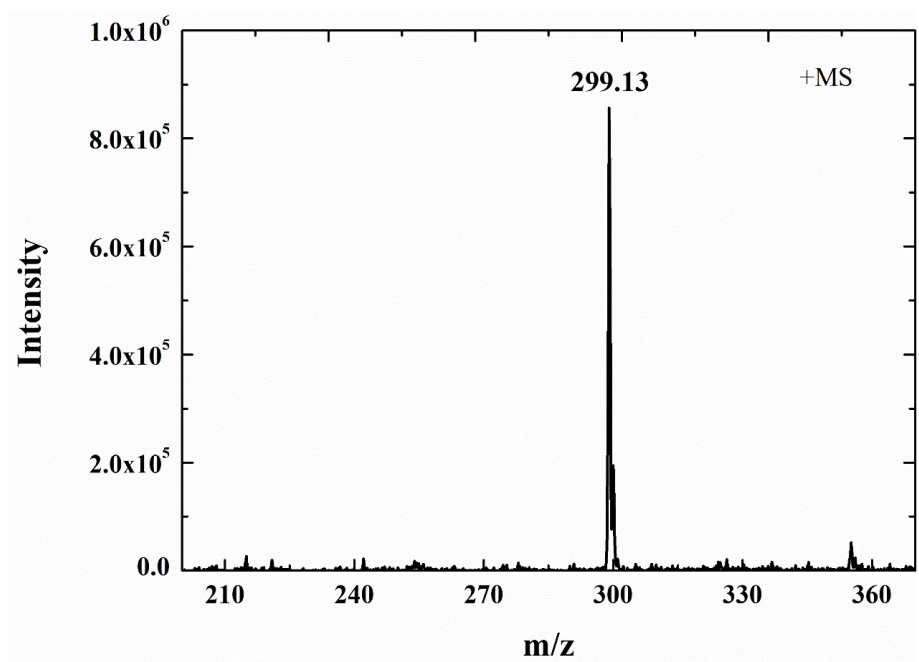
9-PMAH-Pt: IR (KBr): 3781, 3434, 2975, 2274, 1627, 1560, 1527, 1441, 1327, 1260, 1215, 1099, 946, 891, 732, 582 m⁻¹.



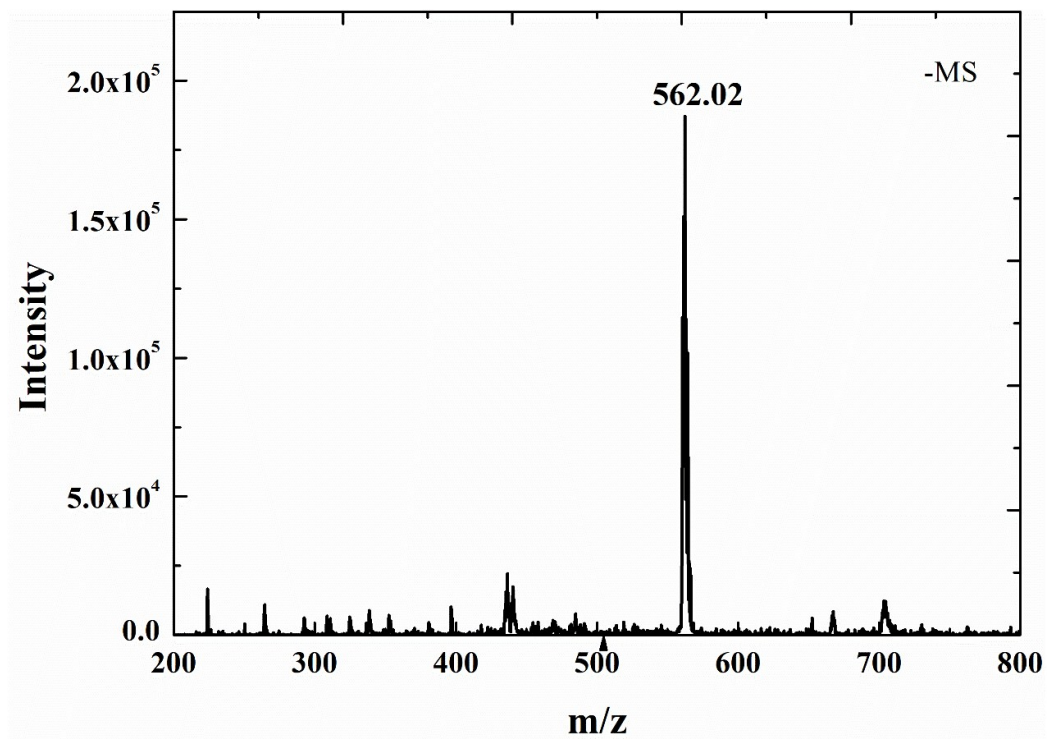
APMAH: IR (KBr): 3424, 2974, 2378, 1582, 1449, 1412, 1050, 757 cm⁻¹



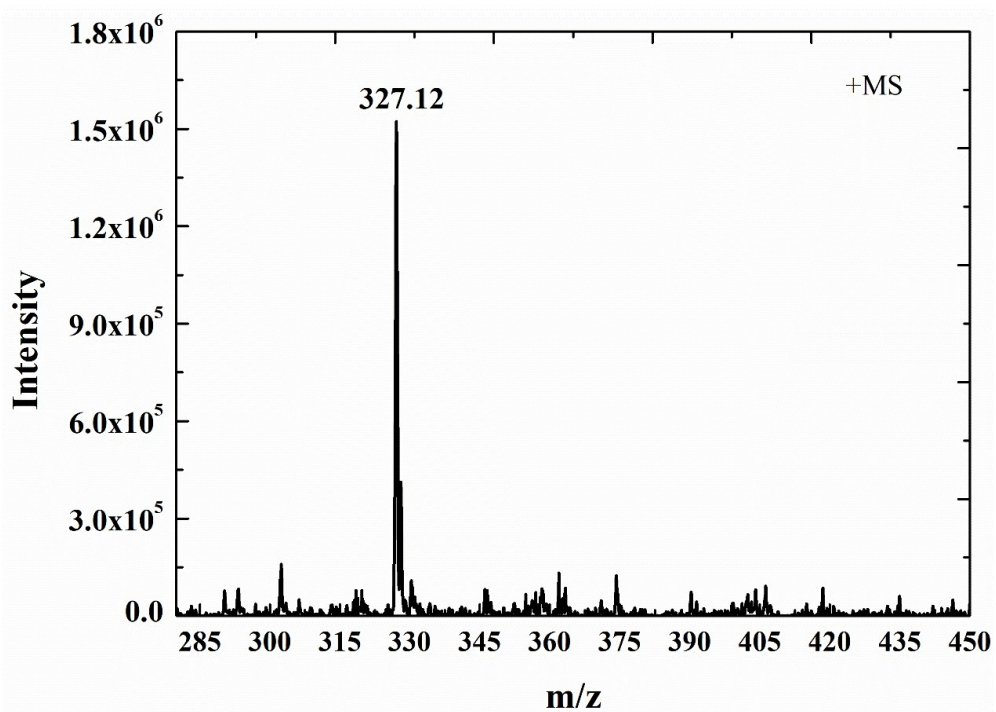
APMAH-Pt: IR (KBr): 3396, 2974, 2892, 1610, 1521, 1440, 1089, 1049, 881, 742 cm⁻¹



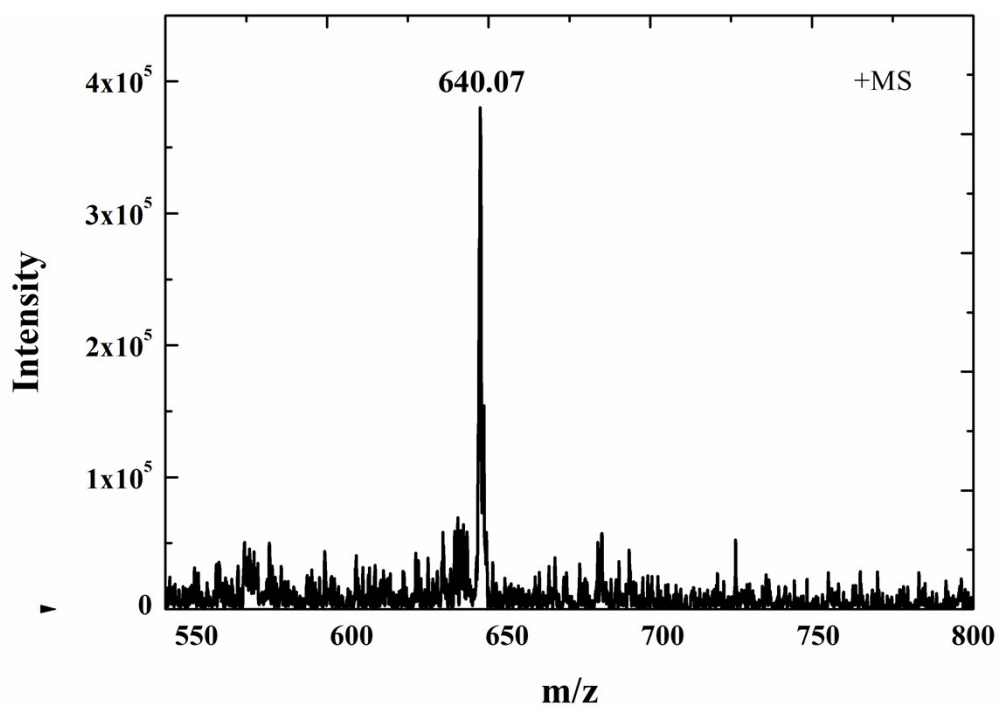
9-PMAH: m/z : 299.13 $[M+H]^+$



9-PMAH-Pt: m/z : 562.02 for $[Pt^{II}Cl_2(9\text{-PMAH})-H]^-$



APMAH: m/z : 327.12 $[M+H]^+$



APMAH-Pt: m/z : 640.07 for $[Pt^{II}Cl_2(APMAH)+EtOH+H]^+$